

## ANALYSIS OF THE APPLICATION OF SiC CERAMICS AS A TOOL MATERIAL IN THE SLIDE BURNISHING PROCESS

### ANALIZA ZASTOSOWANIA CERAMIKI SiC JAKO MATERIAŁU NARZĘDZIOWEGO W PROCESIE NAGNIATANIA ŚLIZGOWEGO

#### Abstract

The paper presents results obtained by SiC ceramic implementation for slide burnishing. Analyses of the effect of the burnishing force and feed on selected surface texture parameters were conducted. The influence of technological parameters was assessed according to the analysis of variance. The burnishing force and feed affected most of the examined surface texture parameters in the analyzed ranges. Optimal values were found for the technological parameters. In most cases, the minimum of height parameters were achieved for 80 N of burnishing force and 0,063 mm/rev of feed. Limitations in the increase in the burnishing force were also found.

**Keywords:** slide burnishing, surface texture, SiC ceramic

#### Streszczenie

W artykule przedstawiono wyniki uzyskane w badaniach nagniatania ślizgowego z zastosowaniem ceramiki SiC. Przeprowadzono analizy wpływu siły nagniatania i posuwu na wybrane parametry struktury geometrycznej powierzchni. Wpływ parametrów technologicznych oceniono na podstawie analizy wariancji. Siła nagniatania i posuw wpłynęły na większość badanych parametrów struktury geometrycznej powierzchni. Wyznaczono optymalne wartości parametrów technologicznych. W większości przypadków minimalne wartości parametrów wysokościowych osiągnęto dla siły nagniatania równej 80 N i przy posuwie równym 0,063 mm/obr. Zidentyfikowano również ograniczenia dotyczące maksymalnej siły nagniatania.

**Słowa kluczowe:** nagniatanie ślizgowe, struktura geometryczna powierzchni, ceramika SiC

## 1. Introduction

Reliability of the automated assembly systems is extremely important. Mounting systems are composed of many elements that work under specific load conditions. One of the factors increasing the durability and reliability of machines and the entire systems is the reliability and durability of their components. The durability of machine elements, depending on the loads, is often significantly influenced by the quality of the surface. Various techniques, e.g. burnishing treatment, can be used to improve the surface quality. Burnishing is used as a final machining of the technological process of parts of machines. The goals of burnishing applications are the increase in fatigue strength, wear resistance, corrosion resistance, dimensional accuracy, kinematic pairs, and others such

as reflection ability. Przybylski [14] defined the burnishing process as the finishing method of the surface when the plastic deformation of the surface layer takes place as a result of interaction between the hard and smooth tool and the processing surface. According to the implementation purpose, the special kind of burnishing, type of tool, and technological parameters range are considered. Slide burnishing is usually applied to smooth the surface by reducing the surface irregularities remained after the prior process. In some cases, changes in the surface layer such as hardening and compressive stress generation caused an increase in fatigue strength, wear, and corrosion resistance. Although the burnishing has many advantages such as machining without chips, high effectiveness of surface smoothing, high safety of

<sup>1</sup> DSc, PhD, Eng. Lidia Gałda, Assoc. Prof. (corresponding author), Rzeszow University of Technology, Faculty of Mechanical Engineering and Aeronautics, 12 Powstańców Warszawy, 35-959 Rzeszów, Poland, Tel. +48 17 8651904, e-mail: lgktmiop@prz.edu.pl, ORCID: 0000-0001-8603-9907.

<sup>2</sup> MSc. Eng. Dariusz Pająk, Rzeszow University of Technology, Faculty of Mechanical Engineering and Aeronautics, 12 Powstańców Warszawy, 35-959 Rzeszów, Poland, Tel. +48 177432456, e-mail: pajak@prz.edu.pl

operating, non-complicated construction of burnishing tools, and others, there are still some disadvantages. Taking into account the plastic deformation effect (in cold conditions) during burnishing, there are several limits in industrial applications. The material of the workpiece should be processable at the surrounding temperature. Another limitation is the stiffness of the system: machine, fixture, workpiece, and tool. Slide burnishing is typically applied to process hard machine parts after the thermal process or with diffusive or galvanic coatings. But it could be used for machine parts of medium or small hardness, especially when the value of burnishing force should be low, such as in processing thin-wall workpieces or objects of small dimensions. In such cases, slide burnishing is an option to finish the surface.

Today, a wide range of hard materials for burnishing tools is emerging starting from different kinds of steel and synthetic diamond ending in special composites. Jaworska et al. [7] worked out the method of direct synthesis of carbon, silicon, and titanium under self-propagating high-temperature synthesis conditions. The diamond composite with  $Ti_3SiC_2$  was used to make cylinder-shaped burnishing tools. Korzyński et al. [12] applied a cylinder-shaped tool of diamond composite tool with a ceramic  $Ti_3SiC_2$  binding phase for slide burnishing. The authors achieved beneficial effects on the fatigue strength of burnished steel elements compared to that of ground workpieces. The increase in fatigue strength was about 18%. Great results in the reduction of the height of the surface texture were presented by Świrad [17]. Due to the application of  $Ti_3SiC_2$  ceramic as a burnishing tool the values of the decrease in the amplitude parameters of surface texture such as Sa, St, and Sz were more than ten times lower than after grinding (without burnishing). Konefał et al. [9] examined the corrosion resistance of stainless steel X6CrNiMoTi17-12-2 and compared the results obtained after different finishing methods. They found that slide burnishing with a spherical diamond tool could improve corrosion resistance, provided that the machined surface has the appropriate texture. Korzyński [10] analyzed a theoretical model of smoothing by the slide burnishing with a tool with a rounding radius of 4 mm and compared it with experimental results. The investigation result made with the application of the low-hardness steel showed good agreement with the results of the model analyses. The author concluded that the post-burnishing surface roughness first of all depended on the pressure force. The optimum burnishing force due to the model was in the range of 25-170 N depending on the hardness, initial surface roughness, and material of the workpiece. The burnishing force obtained experimentally varied from 20 to 150 N depending on other

parameters applied. Radziejewska et al. [15] applied a new hybrid method that combined the laser alloying process and slide burnishing. The authors found that the slide burnishing (with sintered carbides) applied to the alloyed material led to a reduction in surface roughness and the generation of compressive stresses in the surface layer. El-Tayeb et al. [3] carried out ball burnishing on aluminum 6061 with different technological parameters. The authors found values of burnishing force of 160 N and speed of 330 rpm that determine the optimum of surface qualities and tribological properties.

Recently, SiC ceramics were of interest in research in the field of fabrication and special applications of ceramic products. D. Jianxin et al. [8] studied hot pressing of SiC/(W,Ti)C laminated ceramic nozzles. There was the problem of high erosion wear at the nozzle entry area during the sand blasting process. They found that the laminated ceramic nozzles have higher erosion wear resistance than homologous stress-free ceramic nozzles. Researchers have put a lot of effort into improving the properties of porous SiC ceramics. Liu et al. [13] developed the fabrication of cordierite-bonded porous SiC ceramics from  $\alpha$ -SiC,  $\alpha$ - $Al_2O_3$  and MgO using graphite powder as the pore-forming agent. The flexural strength of 26 MPa was achieved at the open porosity of 44,51%. Srivastava et al. [16] applied micrometer-sized SiC,  $Si_3N_4$  and  $Al_2O_3$  particles as reinforcement to Ni based composite. The superior wear resistance exhibited a  $Si_3N_4$  reinforced composite, but there was no significant variation in the friction coefficient for all three composites. Jaworska et al. [6] analyzed the possibility of application by SHS synthesized  $Ti_3SiC_2$  powders as the binding phase for PCD. The authors found that SiC and  $Ti_3SiC_2$  could be sintered by the high-temperature high-pressure method to obtain compacts of the highest hardness of all the analyzed sintering methods. J. Yang et al. investigated a novel  $SiC_{n}/SiC$  composite with nanofibers that is characterized with the maximum flexural strength of 678,2 MPa and the fracture toughness of 8,33  $MPa\ m^{1/2}$  [18].

Nowadays, SiC ceramic is successfully implemented in production of such elements as bearings, nozzles, pistons, and different sliding elements, but there is a few of information about the implementation of SiC ceramic as the burnishing element. Steel of high hardness for balls or rolls are the most common material used in the slide burnishing, but the steel material has the limitations in application for a burnishing element. The adhesive joints and surface deterioration may occurred if the burnishing process is realized with steel burnishing tool-end on steel workpiece.

In this paper, the effect of the implementation of SiC ceramic ball as the burnishing element is presented. The burnishing end of the SiC material characterized high hardness and wear resistance, but the resistance to the fracture toughness resistance is several times smaller than that of steel. This is the limitation of the application of SiC ceramics for specific products. The aim of this study is to examine the possibility of the implementation of SiC ceramic as a burnishing element and the range of technological parameters at which slide burnishing with the SiC ceramic tool is effective. In this paper, the impact analyses of the burnishing technology parameters on selected surface texture parameters are demonstrated.

## 2. Experimental details

### 2.1. Specimens, tool, material, and technological parameters

The material subjected to burnishing process was 42CrMo4 steels. The diameter of the specimen (shaft) was 35 mm. The hardness of the steel after heat treatment was 40 HRC. The surface was formed by a precise turning to a roughness less than Sa 1,2  $\mu\text{m}$ . The burnishing technique was used to finish the surface. The special DB-3 burnishing tool was applied and the SiC ceramic sphere was mounted in the toolholder. The mechanical properties of steel samples and the ceramic spheres of SiC are listed in Table 1.

Table 1. Properties of 42CrMo4 steel and SiC ceramic [2, 19]

| Material | Density         | Hardness        | Coefficient of thermal expansion $\alpha$ | Thermal conductivity | Max temperature of operating | Young modulus | Resistance of fracture toughness |
|----------|-----------------|-----------------|-------------------------------------------|----------------------|------------------------------|---------------|----------------------------------|
| unit     | $\text{g/cm}^3$ | HRC/ HV         | $\times 10^{-6}/\text{K}$                 | W/mK                 | $^{\circ}\text{C}$           | GPa           | $\text{MPa m}^{1/2}$             |
| 42CrMo4  | 7,86            | 40 HRC          | 12                                        | 58                   | 120                          | 200           | 25                               |
| SiC      | 3,12            | 2800 HV (30GPa) | 3                                         | 100                  | 1400                         | 450           | 4                                |

The SEM image of SiC ceramic used for the burnishing element is presented in Fig. 1.

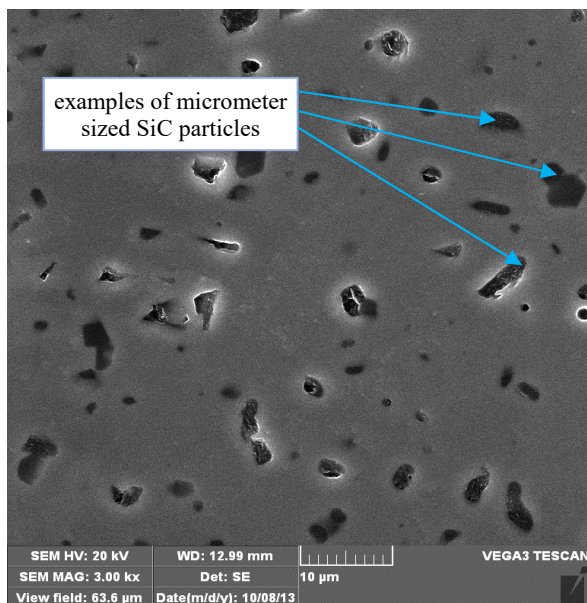


Fig. 1. The SEM image of SiC ceramic (3000x) taken by the VEGA 3 scanning microscope

The burnishing process was performed using a universal lathe type LZ360 (Fig. 2).

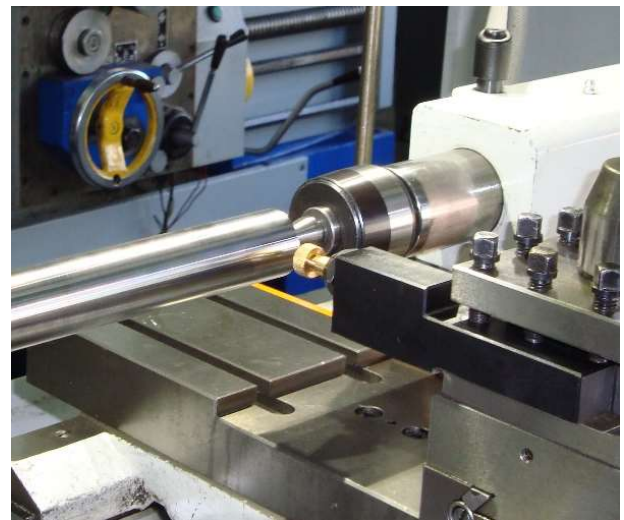


Fig. 2. Photo of the burnishing process

The examined technological parameters were the burnishing force  $P$  [N] and the feed  $f$  [mm/rev]. The burnishing force  $P$  range was 20-200 N with intervals of 20 N, feed  $f$  was in the range of 0,025-0,32 mm/rev in nine steps. The rotational speed  $n$  stayed constant and was equal to 300 rpm. There were three repetitions of each series. The SiC ceramic ball was 6.35 mm in diameter.

## 2.2. Evaluation procedure of the effect of the technological parameters on the surface texture

To assess whether the technological parameters of the burnishing process influence the surface texture, the analysis of variance was used. The influence of each technological parameter was analyzed separately. Analysis of the burnishing force effect was carried out for four levels of 20, 80, 140 and 200 N. The other technological parameters stayed constant, the feed was

equal to 0,04 mm/rev and the rotational speed was 300 rpm. To examine the influence of the feed, the four levels analyze was used too. The feed values were 0,025; 0,063; 0,16 and 0,32 mm/rev and the constant parameters were as follows the burnishing force was equal to 80 N and the rotational speed was 300 rpm. Fifteen parameters of surface texture were chosen in Table 2 that were the output parameters of the slide burnishing process in these analyzes.

Table 2. Description of selected 3D surface texture parameters

| Parameter                         | Description                                                                     |
|-----------------------------------|---------------------------------------------------------------------------------|
| Sp [ $\mu\text{m}$ ]              | Maximum height of peaks                                                         |
| Sv [ $\mu\text{m}$ ]              | Maximum depth of valleys                                                        |
| Sz [ $\mu\text{m}$ ]              | Maximum height of the surface                                                   |
| SHTp [ $\mu\text{m}$ ]            | Surface section height difference corresponding to 20-80% of the material ratio |
| St [ $\mu\text{m}$ ]              | Total height of the surface                                                     |
| Sa [ $\mu\text{m}$ ]              | Arithmetical mean deviation of the surface                                      |
| Sq [ $\mu\text{m}$ ]              | Root mean square deviation of the surface                                       |
| Ssk                               | Skewness of the surface                                                         |
| Sku                               | Kurtosis of the surface                                                         |
| Smr [%]                           | Areal material ratio                                                            |
| Spk [ $\mu\text{m}$ ]             | Reduced peak height                                                             |
| Sk [ $\mu\text{m}$ ]              | Core depth                                                                      |
| Svk [ $\mu\text{m}$ ]             | Reduced valley depth                                                            |
| Sa1 [ $\text{mm}^3/\text{cm}^2$ ] | Peaks volume                                                                    |
| Sa2 [ $\text{mm}^3/\text{cm}^2$ ] | Void volume                                                                     |

All series were measured with the Talysurf CCI Lite white-light interferometer. The area of the measured surfaces was 0,8 mm x 0,8 mm. The repetition of measurements was equal to 3.

Surface texture parameters were calculated using the TalyMap Software.

The analysis of variance is one of many other procedures supporting the selection of significant input parameters of a new process (new tool). The scheme of the overall relation between input and output parameters is presented in Fig. 3.

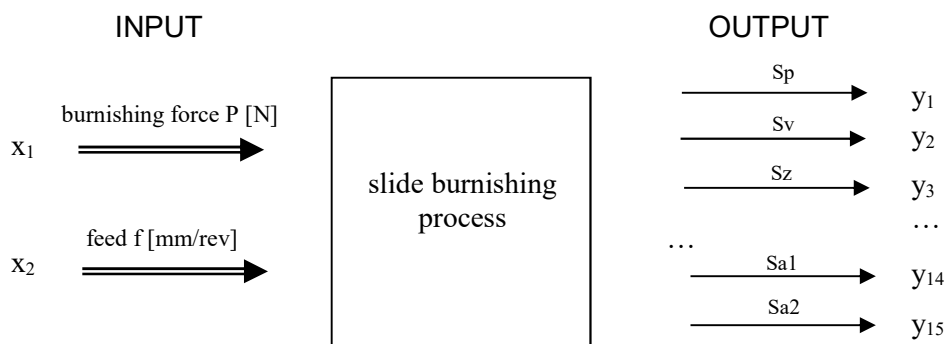


Fig. 3. Scheme of the parameters selected for the input  $x_i$  and output  $y_i$  of the slide burnishing process

The hypothesis that there was no effect of the input technological parameter on the output parameter was analyzed.

Generally, the variance is calculated for selected groups and in this case they are connected with the levels of the technological parameters. The variances

that were obtained between groups and inside groups were compared, and finally the specific test coefficient  $F_t$  was calculated.

The test value  $F_t$  was calculated using the formula [11]:

$$F_t = \frac{\sum_{i=1}^p n_i \cdot (\bar{y}_i - \bar{y})^2 \cdot (n - p)}{\left[ \sum_{i=1}^p \sum_{j=1}^q (y_{ij} - \bar{y})^2 - \sum_{i=1}^p n_i (\bar{y}_i - \bar{y})^2 \right] \cdot (p - 1)}$$

The test coefficient  $F_t$  was compared to the critical value  $F_{cr}$  found in the Fisher-Snedecor table for the importance level  $\alpha$  of 0,05.

Confirmation or cancellation the hypothesis is based on the comparison of the values of  $F_t$  and  $F_{cr}$ . If  $F_t \geq F_{cr}$ , the assumed hypothesis should be cancelled, which means that the input parameter evidently influenced the output parameter. Otherwise, if  $F_t < F_{cr}$ , the hypothesis is confirmed and there was no effect of the input parameter on the output parameter in the investigated range.

Additionally, the average values of surface texture parameters were compared between series and to zero series (after precise turning).

The SiC ceramic spheres were examined after the burnishing process to review the wear in the contact

zone. Photos of the contact zone of the SiC ball were taken with the optical microscope Neophot2.

### 3. Results and discussion

In Fig. 4 a view of the exemplified surface after precise turning is presented. The periodic anisotropic deterministic surface was created with regular traces after the turning process.

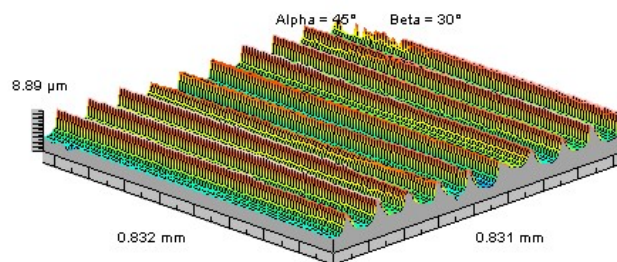


Fig. 4. The isometric view of the surface after precise turning

Figure 5 presents views of burnished surfaces using the tool with the SiC ceramic sphere in the range of burnishing force  $P_i = 20 - 200$  N.

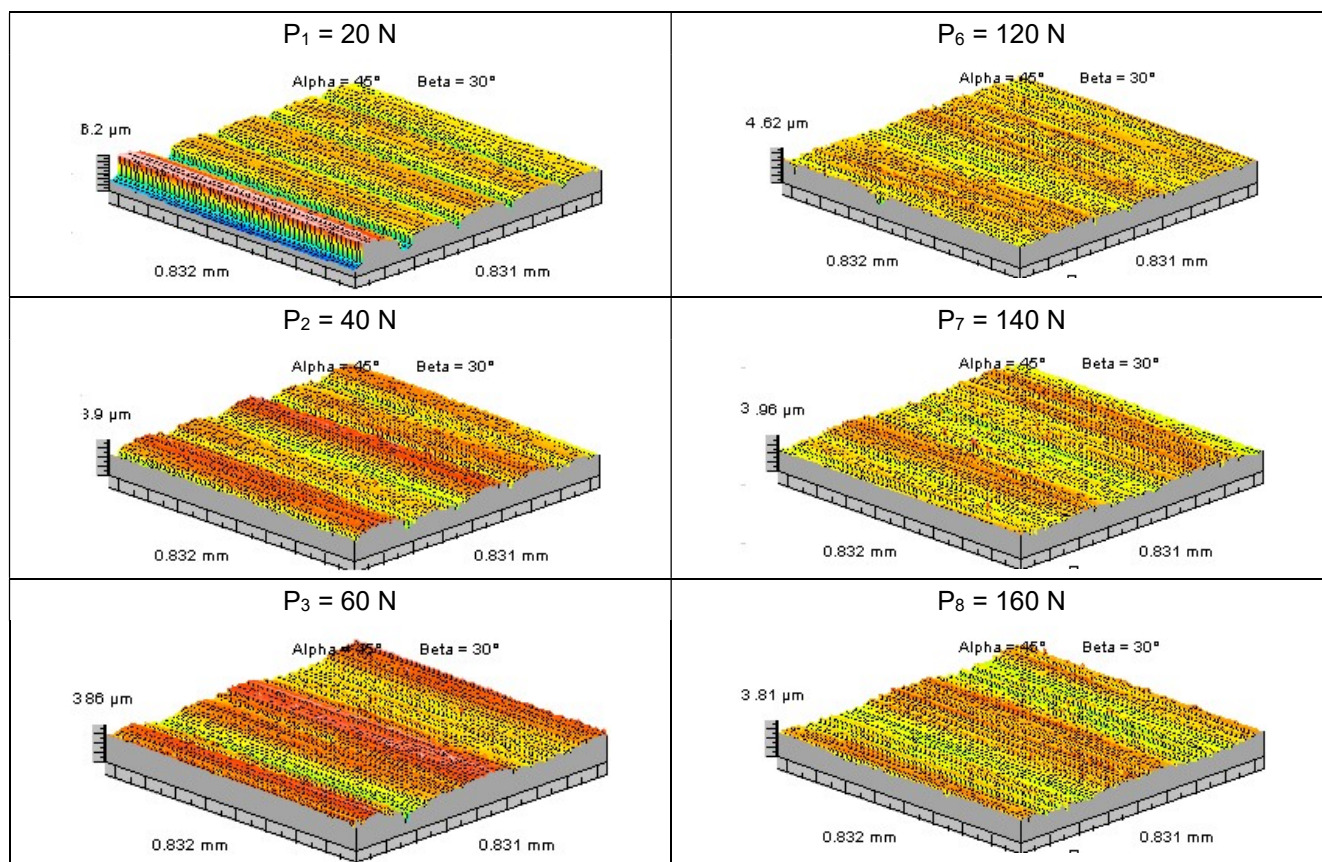


Fig. 5. Isometric views of surfaces burnished by the tool with SiC ceramic sphere in the range of burnishing force  $P_i = 20 - 200$  N

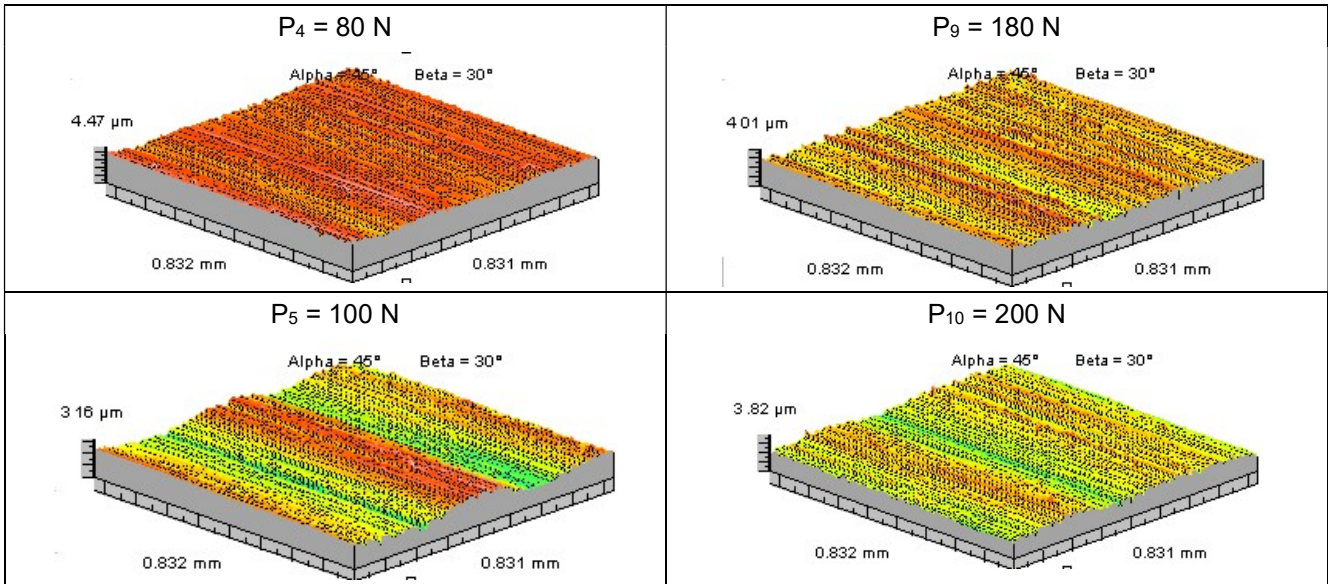


Fig. 5 (cont.). Isometric views of surfaces burnished by the tool with SiC ceramic sphere in the range of burnishing force  $P_i = 20 - 200$  N

The analyses of the views of the surfaces and the surface texture parameters (Table 3) demonstrated that the slide burnishing with the SiC ceramic could be a useful method to process the surface. It can be observed that at low burnishing force  $P_i$  in the range of 20-60 N valleys formed in precise turning were still on the surface, but the peaks were strongly flattened. At the burnishing force  $P$  equal to 80 N, the surface was the

smoothest of all examined. As a result of burnishing, most of the surface height parameters decreased. The average values of the surface texture parameters for each surface burnished with SiC ceramic at the burnishing force  $P_i$  in the range of 20-200 N and the relevant – without burnishing – are presented in Table 3.

Table 3. The average values of surface texture parameters for each surface burnished with SiC ceramic at the burnishing force  $P_i$  in the range of 20-200 N

| Parameter                         | Average value of surface texture parameters at burnishing force $P_i$ [N] |       |             |             |       |             |       |              |             |       |        |
|-----------------------------------|---------------------------------------------------------------------------|-------|-------------|-------------|-------|-------------|-------|--------------|-------------|-------|--------|
|                                   | 20                                                                        | 40    | 60          | 80          | 100   | 120         | 140   | 160          | 180         | 200   | turned |
| Sp [ $\mu\text{m}$ ]              | 2,16                                                                      | 2,87  | 1,25        | <b>1,14</b> | 1,42  | 3,88        | 1,39  | 1,38         | 2,79        | 1,60  | 5,99   |
| Sv [ $\mu\text{m}$ ]              | 3,54                                                                      | 3,80  | 3,45        | <b>2,09</b> | 2,18  | 2,57        | 2,49  | 2,28         | 2,40        | 2,88  | 3,94   |
| Sz [ $\mu\text{m}$ ]              | 5,07                                                                      | 6,65  | 4,49        | <b>3,22</b> | 3,58  | 6,44        | 3,88  | 3,66         | 5,20        | 4,75  | 9,93   |
| SHTp [ $\mu\text{m}$ ]            | 0,76                                                                      | 0,63  | 0,61        | 0,43        | 0,50  | 0,43        | 0,48  | 0,54         | <b>0,41</b> | 0,52  | 2,50   |
| St [ $\mu\text{m}$ ]              | 5,07                                                                      | 6,67  | 4,71        | <b>3,22</b> | 3,60  | 6,44        | 3,88  | 3,66         | 5,20        | 4,75  | 9,93   |
| Sa [ $\mu\text{m}$ ]              | 0,45                                                                      | 0,34  | 0,29        | 0,23        | 0,25  | 0,25        | 0,23  | 0,25         | <b>0,20</b> | 0,25  | 1,19   |
| Sq [ $\mu\text{m}$ ]              | 0,65                                                                      | 0,46  | 0,36        | 0,30        | 0,31  | <b>0,28</b> | 0,30  | 0,31         | 0,26        | 0,32  | 1,47   |
| Ssk                               | <b>-1,14</b>                                                              | -1,30 | -0,76       | -0,70       | -0,54 | -0,58       | -0,56 | -0,27        | -0,36       | -0,59 | 0,93   |
| Sku                               | 4,75                                                                      | 5,78  | 5,16        | 4,13        | 3,76  | 4,96        | 4,20  | <b>3,11</b>  | 5,95        | 3,90  | 2,86   |
| Smr [%]                           | 45,03                                                                     | 4,10  | 28,17       | 25,37       | 11,83 | <b>0,03</b> | 8,47  | 13,92        | 7,32        | 1,70  | 1,28   |
| Spk [ $\mu\text{m}$ ]             | 0,32                                                                      | 0,19  | <b>0,17</b> | 0,24        | 0,21  | 0,20        | 0,19  | 0,21         | 0,23        | 0,24  | 2,90   |
| Sk [ $\mu\text{m}$ ]              | 0,79                                                                      | 0,90  | 0,92        | 0,72        | 0,77  | 0,65        | 0,75  | 0,83         | <b>0,62</b> | 0,76  | 2,37   |
| Svk [ $\mu\text{m}$ ]             | 0,96                                                                      | 0,89  | 0,46        | 0,39        | 0,40  | 0,44        | 0,39  | <b>0,30</b>  | 0,32        | 0,42  | 0,43   |
| Sa1 [ $\text{mm}^3/\text{cm}^2$ ] | 33,85                                                                     | 6,93  | <b>5,87</b> | 12,39       | 9,06  | 7,72        | 7,57  | 8,74         | 10,53       | 8,22  | 376,67 |
| Sa2 [ $\text{mm}^3/\text{cm}^2$ ] | 102,30                                                                    | 70,50 | 25,93       | 21,43       | 24,17 | 28,60       | 21,17 | <b>16,23</b> | 19,00       | 29,77 | 11,86  |

Most of the surface texture parameters analyzed decreased after the burnishing process with a force in the range of 20 to 200 N. The height parameters Sz and St decreased from 32 to 67%, but this was mainly due to the flattening of the peaks during burnishing. It confirmed a superior decrease in the maximum height

of the summits Sp which was in the range of 35-80% compared to a decrease in Sv of 3-46% depending on the burnishing force value used. The mean amplitude parameters showed smaller values of approximately 62-83% for Sa parameter and 55-82% for Sq parameter. A similar tend was observed for the surface

section height difference SHTp and the average decrease was approximately 75% (the range of 69-83%). Quite different changes were obtained in the case of the Smr parameter that corresponds to the material ratio. The values of the Smr decrease was about 97%, but the increase was even of 3417% compared to turned surfaces. The Smr parameter values showed odd performance with increasing burnishing force and compared to changes in other measured surface texture parameters. Skewness of all burnished surfaces became negative (Ssk in the range from -1,14 to -0,27) and the decrease was significant of 125% on average compared to non-burnished samples. The surface kurtosis after burnishing increased in all series, but the range of values was quite wide. The increase in Sku ranged from 8 to 108%. The changes in Sk family parameters were very interesting for analyzing the effect of the increasing force on the surface geometry. Parameters corresponded to the summits of the surfaces Spk and Sa1 decreased with increasing force, and the change in values was significant 92% and 94% on average, respectively. The scatter of values changes was rather narrow 88-94% of Spk and 91-98% of Sa1. The decrease in peaks height and volumes proved that the plastic deformation of the summits was successful. As a result of burnishing, the core depth Sk was smaller than that of turned surfaces of about 66% on average. Values of the Svk parameter with the increase in burnishing force increasing to 60 N were greater than those of the turned surfaces (even 123%), but then from the burnishing force of

80 N the Svk parameter was usually lower and oscillated around 0,4  $\mu\text{m}$  for higher burnishing forces. The maximum decrease was 30% of the Svk parameter. Taking into account the changes of void volumes Sa2 of the burnishing surfaces, we can observe a great increase ranging from 36-762% although the reduced valley depth decreased at higher burnishing forces. This was because a new surface geometry was created during the burnishing process with higher force. The burnishing tool had different geometry than the turning one, and the burnishing sphere left the shallow and smooth traces on the surface instead of deep and sharp after the turning process.

To analyze the effect of the burnishing force on the surface texture parameters, four levels of  $P_i$  were selected: minimum  $P_1 = 20$  N,  $P_2 = 80$  N as the most height parameters reached their minimum,  $P_3 = 140$  N and maximum  $P_4 = 200$  N. The critical value  $F_{cr}$  for 4 levels, 3 repetitions and importance level of 0,05 amounted to 4,06 (Fisher-Snedecor statistics). Using the analysis of variance procedure, it was found that the burnishing force  $P$  in the range of 20-200 N had an effect on 11 of the 15 texture parameters analyzed. The burnishing force influenced the surface texture parameters from different groups: height Sp, Sv, Sz, St, mean Sa, Sq, connected with the material ratio SHTp, Smr, skewness Ssk, and from Sk family: Svk and Sa2. The graphs of the relationship between the increase in burnishing force  $P$  and the selected texture parameters on which the effect was significant are presented in Fig. 6.

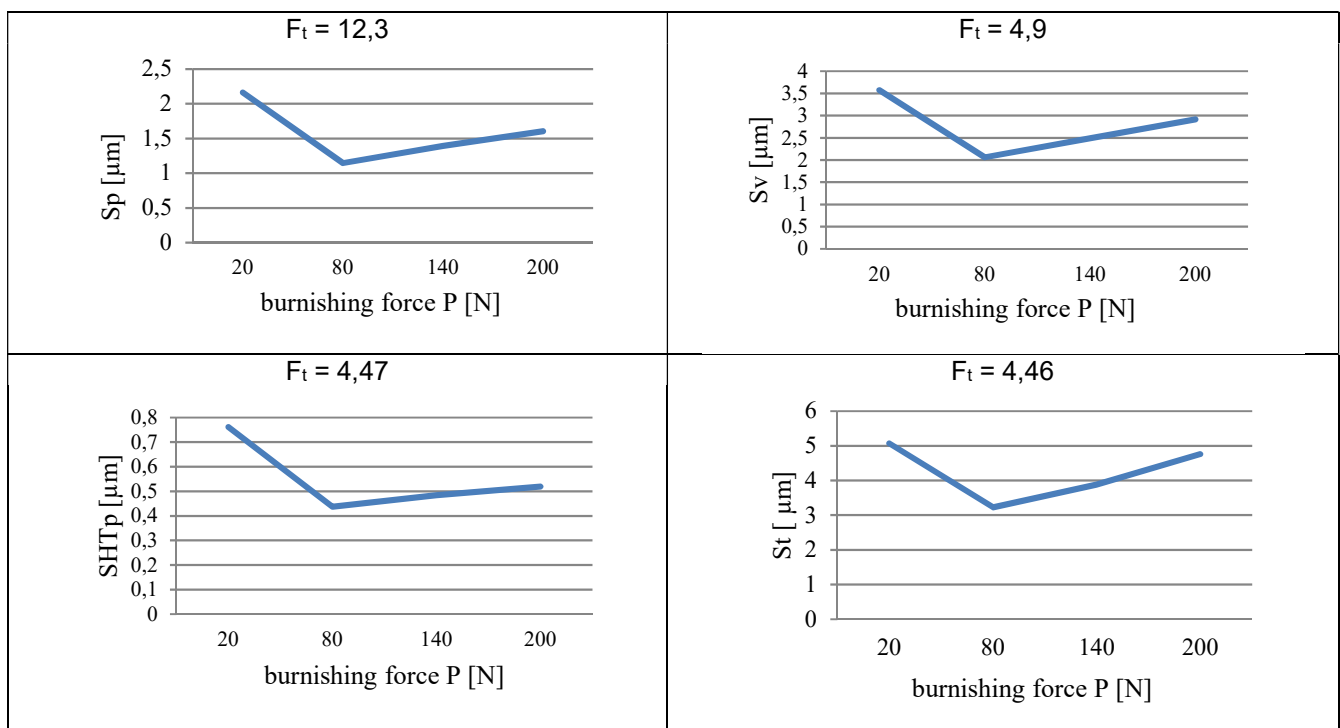


Fig. 6. Relations between the burnishing force  $P$  and the selected texture parameters

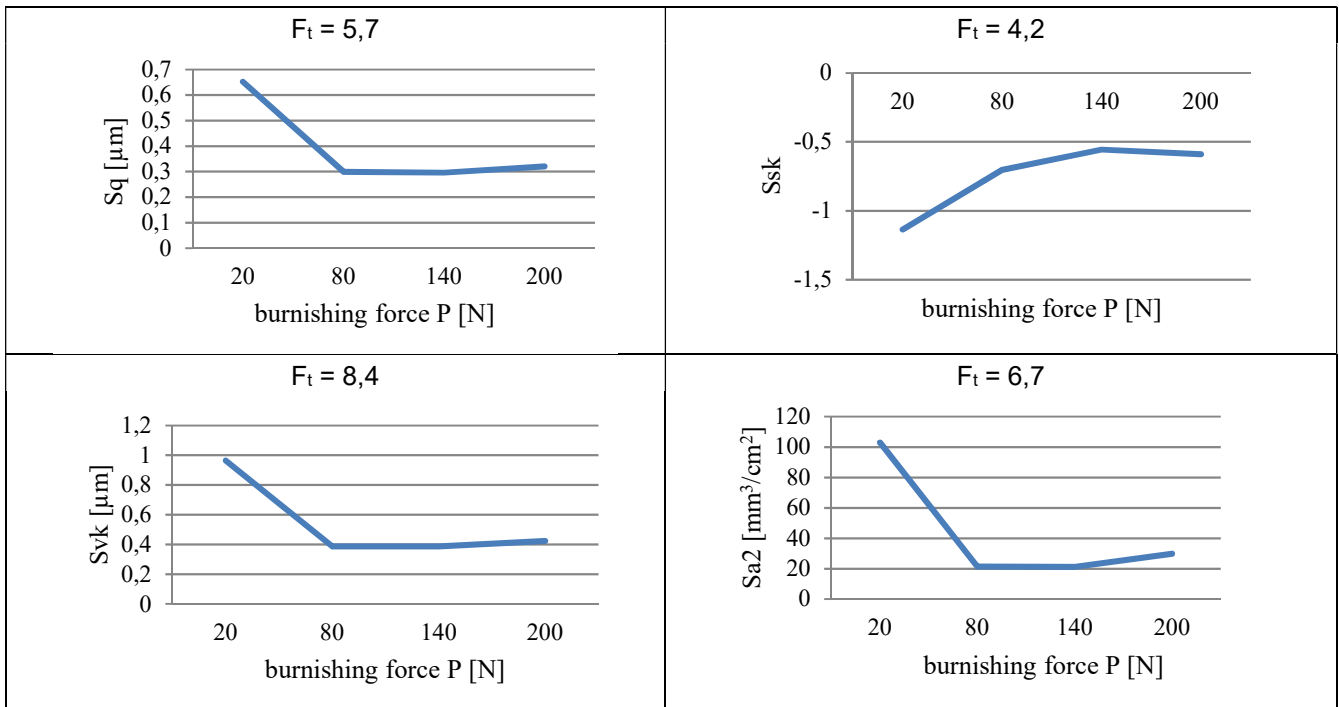


Fig. 6 (cont.). Relations between the burnishing force P and the selected texture parameters

Analyzing the curves, the extreme points can be observed. Minimum values of most surface texture parameters were obtained for a burnishing force of 80 N. The exception was the maximum value of the Ssk parameter when the force was equal to 140 N and for the whole range of force values the skewness remained negative. Significant changes in the surface texture parameters values of the burnished surfaces were obtained when the burnishing force was in the range of 20 to 80 N. Most of the parameters decreased at least by 36% (St) with increasing force to 80 N. Generally, height parameters decreased by about 40%, mean parameters decreased by 55% on average, and the greatest decrease was observed in the void volume of 80%. With the increase of the burnishing force over 80 N values of texture parameters started to enlarge but this growth was not so big, mostly it was about a few percent. Exceptions were the total height of the surface

St and, as a consequence, the maximum height of summits and depth of valleys. At the maximum burnishing force 200 N, they reached almost the same values that were obtained at 20 N. That denoted that there was no need to increase the burnishing force to over 200 N. Comparing results obtained with the SiC burnishing tool to the outcome of the burnishing process with typical steel tool, one may conclude that the quality of the burnished surface after processing with the SiC ceramic sphere is much better than obtained by steel burnishing element [4]. Additionally, taking into account the good tribological performance of the SiC element [1, 5], the new material tool could be a good alternative to the steel.

The influence of feed on surface texture parameters was also analyzed. Fig. 7 presents views of burnished surfaces using the tool with a SiC ceramic sphere with feed  $f_i$  in the range of 0,025-0,32 mm/rev.

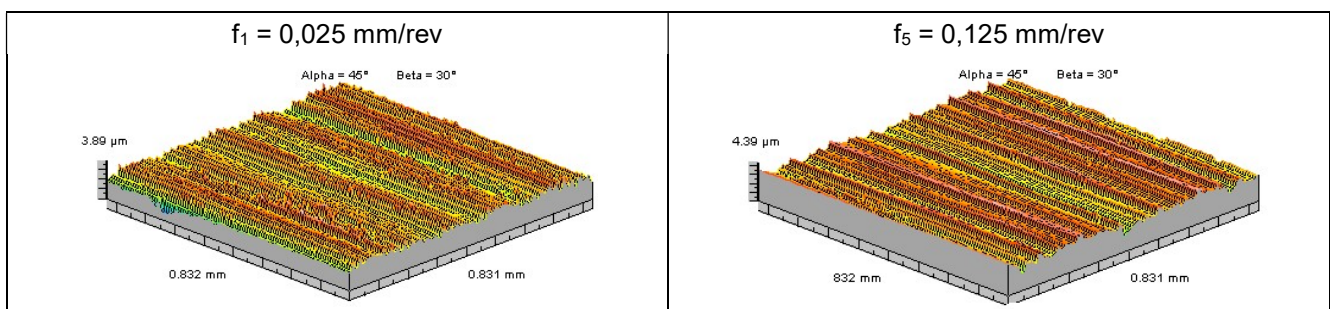


Fig. 7. Isometric views of surfaces burnished by the tool with a ceramic sphere of SiC in the feed range  $f_i = 0,025 - 0,32$  mm/rev



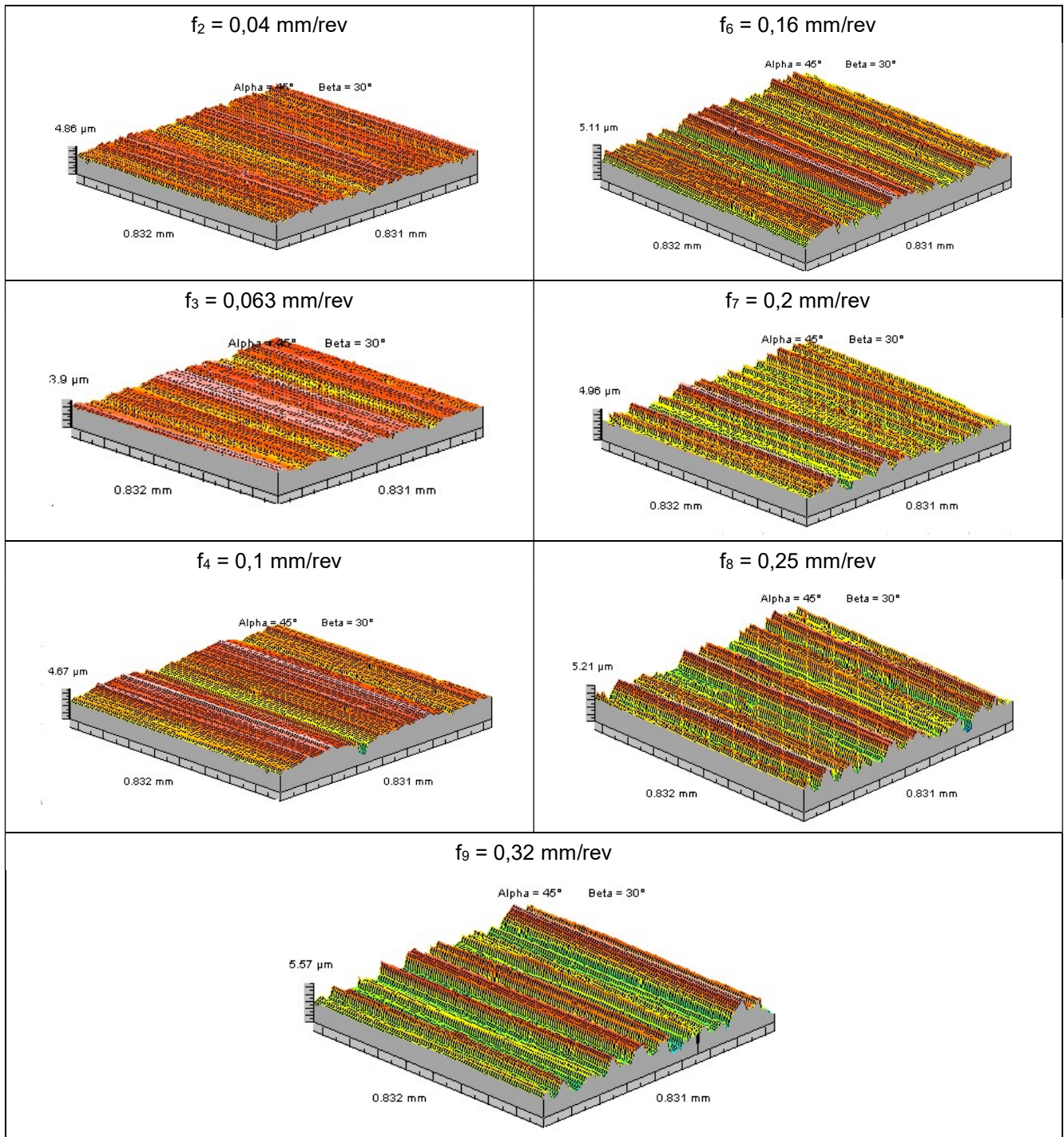


Fig. 7 (cont.). Isometric views of surfaces burnished by the tool with a ceramic sphere of SiC in the feed range  $f_i = 0,025 - 0,32$  mm/rev

The one directional lay of the surfaces was obtained after slide burnishing with a SiC ceramic sphere in the examined range of feed from 0,025 to 0,32 mm/rev. Clear traces of the burnishing sphere pass were visible on the processing surfaces starting from the feed of 0,125 mm/rev. This is typical because with increasing feed, the traces of machining are more observable because of greater distance between them.

With increasing feed, the height of surface texture increased but was lower compared to that after turning (Fig. 4).

In Table 4 the average values of surface texture parameters after the burnishing with SiC ceramic with the feed in the range of 0,025-0,32 mm/rev and the relevant values – from the surface without the burnishing are presented.

Table 4. The average values of surface texture parameters for surfaces burnished with SiC ceramic at feed in the range of 0,025-0,32 mm/rev

| Parameter                         | Average value of surface texture parameters at feed $f_i$ [mm/rev] |       |              |       |       |       |       |       |             |        |
|-----------------------------------|--------------------------------------------------------------------|-------|--------------|-------|-------|-------|-------|-------|-------------|--------|
|                                   | 0,025                                                              | 0,04  | 0,063        | 0,1   | 0,125 | 0,16  | 0,2   | 0,25  | 0,32        | turned |
| Sp [ $\mu\text{m}$ ]              | 1,42                                                               | 1,40  | <b>1,16</b>  | 1,27  | 1,49  | 1,69  | 1,83  | 2,14  | 2,85        | 5,99   |
| Sv [ $\mu\text{m}$ ]              | <b>1,84</b>                                                        | 2,68  | 2,85         | 2,88  | 2,74  | 2,94  | 2,86  | 3,38  | 2,79        | 3,94   |
| Sz [ $\mu\text{m}$ ]              | <b>2,95</b>                                                        | 4,08  | 4,02         | 3,70  | 3,92  | 4,52  | 4,63  | 5,31  | 5,65        | 9,93   |
| SHTp [ $\mu\text{m}$ ]            | 0,59                                                               | 0,55  | <b>0,46</b>  | 0,54  | 0,65  | 0,82  | 1,02  | 1,16  | 1,39        | 2,50   |
| St [ $\mu\text{m}$ ]              | <b>3,26</b>                                                        | 4,08  | 4,02         | 4,15  | 4,24  | 4,62  | 4,69  | 5,52  | 5,65        | 9,93   |
| Sa [ $\mu\text{m}$ ]              | 0,28                                                               | 0,26  | <b>0,24</b>  | 0,29  | 0,32  | 0,40  | 0,47  | 0,58  | 0,63        | 1,19   |
| Sq [ $\mu\text{m}$ ]              | 0,34                                                               | 0,33  | <b>0,33</b>  | 0,39  | 0,42  | 0,51  | 0,59  | 0,74  | 0,77        | 1,47   |
| Ssk                               | 0,09                                                               | -0,44 | <b>-1,20</b> | -0,75 | -0,33 | -0,23 | 0,09  | -0,16 | 0,26        | 0,93   |
| Sku                               | 2,80                                                               | 3,62  | 5,71         | 5,24  | 3,69  | 3,21  | 2,85  | 3,01  | <b>2,46</b> | 2,86   |
| Smr [%]                           | 12,60                                                              | 11,85 | 18,87        | 23,70 | 11,67 | 9,52  | 9,35  | 6,58  | 2,46        | 1,28   |
| Spk [ $\mu\text{m}$ ]             | 0,30                                                               | 0,23  | <b>0,18</b>  | 0,36  | 0,40  | 0,44  | 0,56  | 0,65  | 0,73        | 2,90   |
| Sk [ $\mu\text{m}$ ]              | 0,89                                                               | 0,82  | <b>0,64</b>  | 0,83  | 0,96  | 1,27  | 1,45  | 1,78  | 1,88        | 2,37   |
| Svk [ $\mu\text{m}$ ]             | <b>0,28</b>                                                        | 0,39  | 0,59         | 0,72  | 0,60  | 0,63  | 0,53  | 0,73  | 0,67        | 0,43   |
| Sa1 [ $\text{mm}^3/\text{cm}^2$ ] | 17,87                                                              | 10,21 | <b>7,15</b>  | 16,50 | 21,47 | 23,87 | 37,60 | 39,10 | 62,10       | 376,67 |
| Sa2 [ $\text{mm}^3/\text{cm}^2$ ] | <b>12,85</b>                                                       | 25,97 | 48,13        | 41,63 | 35,30 | 31,30 | 24,33 | 43,33 | 22,06       | 11,86  |

Most of the surface texture parameters analyzed decreased due to the burnishing process. Eight out of fifteen parameters analyzed got their minimum with a feed of 0,063 mm/rev. There were mainly height but related with summit parameters. Six parameters reached minimum values at the lowest feed of 0,025 mm/rev. That parameters were associated with height of surface and valley dimensions created during the burnishing process. Compared to turning surfaces, the decrease in mean parameters was in the range of 47-80% (Sa and Sq). Similar changes were found in relation to height parameters such as Sp, Sz, St, and SHTp, but the decrease in the Sv values was smaller and varied from 14 to 53%. The parameter Svk related to the surface valley but to reduced depth presented both the increase and decrease compared to Svk of the turned surfaces. The changes in surface texture created during slide burnishing in such a feed range were more evident when one looked at the void volume Sa2 of the processing surfaces. The volume of the void increased in a very wide range of 8% to more than 300% although the maximum depth of the valleys declined at all feeds in the set. It is connected with changes in the skewness and kurtosis of the surfaces. Although the value of the Ssk parameter decreased in the range of 72-230% some of them remained positive. Sku values were usually larger than that after turning even over 100%, but there were some that slightly decreased. The reduced summit heights and summit volumes decreased significantly by at least 75% to almost 100% as a result of flattening the peaks and due to the shape of the burnishing SiC sphere. Core depths were lower than after turning at the whole range of burnishing feed. The values of the Smr parameter increased

considerably and the changes were in a large range of 92-1751%.

The analysis of variance was used to analyze the effect of the feed on the surface texture parameters in the burnishing process. As for the burnishing force, four levels of feed  $f_i$  were selected: minimum  $f_1 = 0,025$  mm/rev,  $f_2 = 0,063$  mm/rev because the most of the surface texture parameters reached their minimum,  $f_3 = 0,16$  mm/rev and maximum  $f_4 = 0,32$  mm/rev. There were 3 repetitions at each level and the critical value  $F_{cr}$  was equal to 4,06. It was found that the feed  $f$  in the range of 0,025-0,32 mm/rev had influenced 14 of the 15 texture parameters of the surface studied. Statistically, it was not revealed that the feed affected only Sa2 from Sk family. The graphs of the relationship between increasing feed  $f$  and selected texture parameters on which the effect were significant are shown in Fig. 8.

From all graphs presented in Fig. 8 only the values of the Sz parameter showed continuous growth with increasing feed. Usually, the minimum parameters values were obtained at 0,063 mm/rev and in the case of kurtosis of the surface, the maximum point was reached. Increasing the feed from 0,025 mm/rev to 0,063 mm/rev resulted in a decrease in the maximum height of the summits of 18% and also in the reduced summit height over 40%. Similar tendency was observed in surface parameters connected with core depth. The smallest decrease was obtained for the mean parameter Sa of 14%. From an economic reason it is more profitable to process at higher velocity, but according to quality assurance standards the surface characteristics should qualify the client's demands. A beneficial result was obtained of the surface

skewness because the Ssk value decreased considerably to negative -1,2, whereas kurtosis of the surface increased over twice. A further increase in feed greater

than 0,063 mm/rev caused surface deterioration and the values of all the parameters analyzed except the surface kurtosis increased even several times.

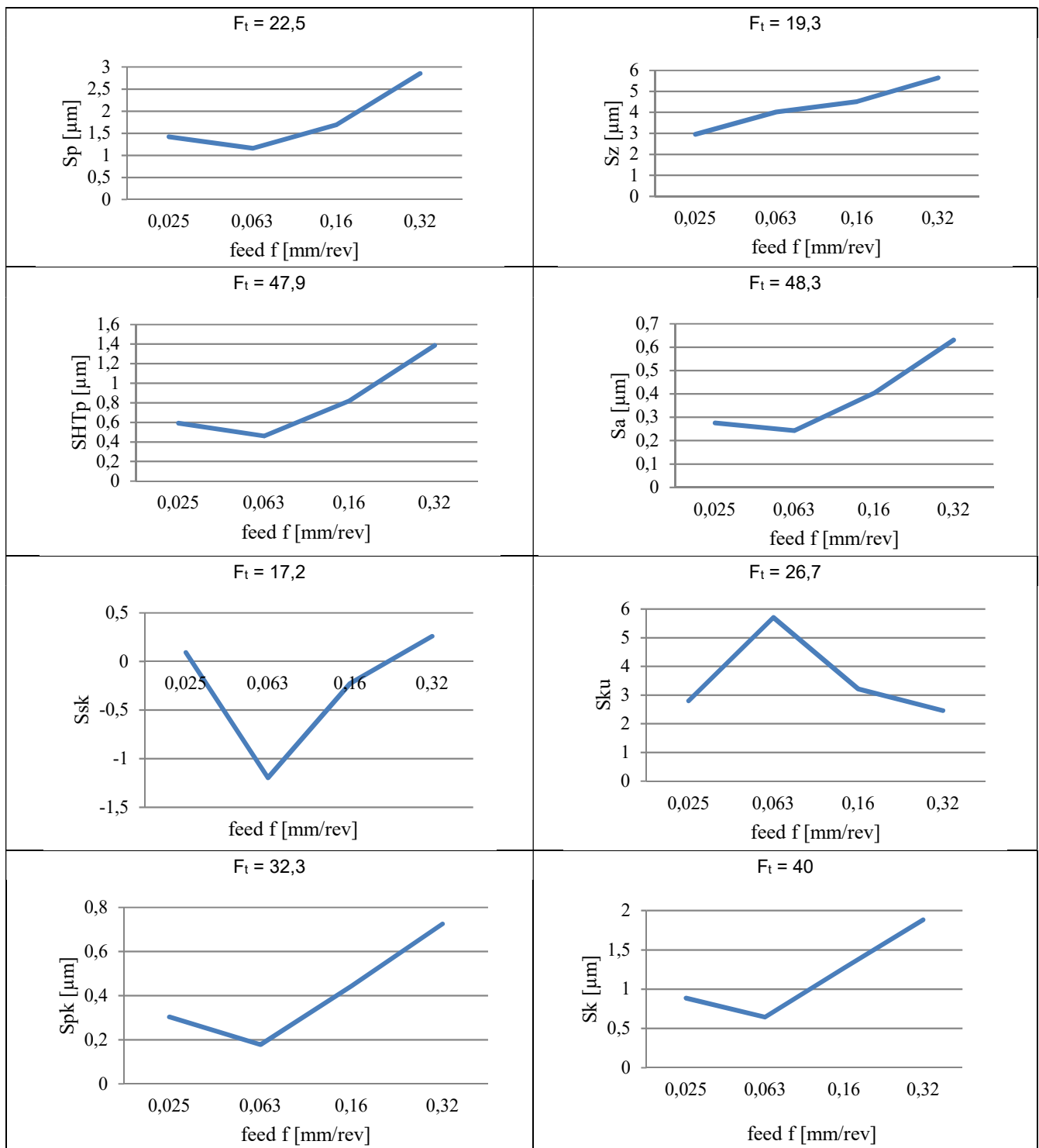


Fig. 8. Relationship between the feed f and the selected texture parameters

In order to find the maximum force P (limitation burnishing force) for the slide burnishing process with SiC ceramic in this application, a further increase in P was realized. During burnishing at P equal to 220 N, the dark abrasive wear debris from the SiC element

were observed and the process was stopped. The surface of the burnishing element was subjected to observation. The contact zone of the SiC ball is presented in Fig. 9.

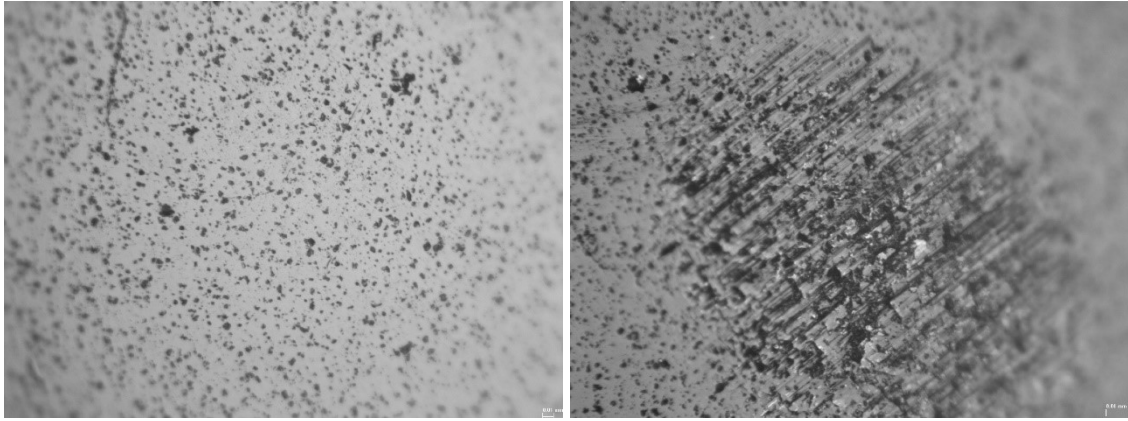


Fig. 9. Photos (x200) of the contact zone of the SiC ball before (left) and after the slide burnishing with  $P = 220$  N (right)

There are visible scratches in the contact zone of the SiC ceramic ball after burnishing process with force  $P$  of 220 N. The ball surface was interrupted where abrasive wear occurred. This was caused because of the low resistance of fracture toughness as a consequence of the low shear resistance. During slide burnishing between two elements: working ending and processed workpiece, the force system was constituted. Then the roughness deformation took place due to the simultaneous action of normal and shear forces. Because the hardness of the workpiece was much lower, the changes in the surface roughness and performance concern the processed steel, but at 220 N of burnishing force, the abrasive wear occurred on the SiC ceramic tool end. It means that the value of the burnishing force of 220 N for the slide burnishing process is too high in this application. Further detailed examination of the tool life with SiC ceramic is needed.

#### 4. Conclusions

The opportunity of using SiC ceramic as a burnishing tool was examined. It was discovered that the burnishing force and feed influenced the most analyzed surface texture parameters. The ranges of selected technological parameters at which effective processing is possible were found. For slide burnishing the surface of 42CrMo4 steel with SiC sintered ceramic ball of 6,35 mm in diameter, the burnishing force  $P$  should not exceed 200 N. The best results in smoothing the surface were achieved at 80 N of burnishing force and 0,063 mm/rev of feed. The values of the amplitude parameters  $S_a$  and  $S_q$  were five times smaller after slide burnishing at  $P$  equal to 80 N compared to the non-burnished surface. Height parameters decreased at least several times,  $S_p$  five times,  $S_t$  three times,  $S_v$  almost two times, and some parameters such as reduced summit height declined over twelve times. It confirms that there is a potential

in the application of SiC ceramic as tool material in the burnishing process.

#### References

- [1] Bulikowska B., Gałda L. 2015. "The effect of surface roughness on the tribological properties of sliding elements in material assembly SiC-42CrMo4". *TRIBOLOGIA*, XLVI(4): 21-31.
- [2] Dobrzański A. L. 2008. *Non-metallic engineering materials*. Gliwice: Publishing house of Silesian University of Technology.
- [3] El-Tayeb N.S.M., Low K.O., Brevern P.V. 2009. "On the surface and tribological characteristics of burnished cylindrical Al-6061". *Tribology International* 42: 320-326.
- [4] Gałda L. 2014. Slide burnishing with ceramic material. In *Contemporary problems in the technology of burnishing*, 143-154. Publishing house of Gdańsk University of Technology.
- [5] Gałda L. 2016. "Selected factors effecting on wear resistance of sliding pairs". *BUSES – technology, operations, transport systems* 17: 861-865.
- [6] Jaworska L., Sobierski L., Twardowska A., Królicka D. 2005. „Preparation of materials based on Ti-Si-C system using high temperature-high pressure method”. *Journal of Materials Processing Technology* 162-163: 184-189.
- [7] Jaworska L., Szutkowska M., Morgiel M., Sobierski L., Lis J. 2001. „Ti3SiC2 as a bonding phase in diamond composites”. *Journal of Materials Science Letters* 20: 1783-1786.
- [8] Jianxin D., Lili L., Mingwei D. 2007. „Erosion wear behaviours of SiC/(W,Ti)C laminated ceramic nozzles in dry sand blasting processes”. *Materials Science & Engineering A* 444: 120-129.
- [9] Konefał K., Korzyński M., Byczkowska Z., Korzyńska K. 2013. „Improved corrosion resistance of stainless steel X6CrNiMoTi17-12-2 by slide diamond burnishing”. *Journal of Materials Processing Technology* 213: 1997-2004.
- [10] Korzyński M. 2009. "A model of smoothing slide ball-burnishing and an analysis of the parameter interaction". *Journal of Materials Processing Technology* 209: 625-633.
- [11] Korzyński M. 2013. *Experiment design*. Warszawa: Scientific publishing house PWN.

- [12] Korzyński M., Lubas J., Świrad S., Dudek K. 2011. „Surface layer characteristics due to side diamond burnishing with a cylindrical-ended tool”. *Journal of Materials Processing Technology* 211: 84-94.
- [13] Liu S., Zeng Y.-P., Jiang D. 2009. “Fabrication and characterization of cordierite-bonded porous SiC ceramics”. *Ceramics International* 35: 597-602.
- [14] Przybylski W. 1987. *Burnishing technology*. Warszawa: Science Publishing House.
- [15] Radziejewska J., Skrzypek S.J. 2009. „Microstructure and residual stresses in surface layer of simultaneously laser alloyed and burnished steel”. *Journal of Materials Processing Technology* 209: 2047-2056.
- [16] Srivastava M., Grips V.K.W., Rajam K.S. 2008. “Influence of SiC, Si<sub>3</sub>N<sub>4</sub> and Al<sub>2</sub>O<sub>3</sub> particles on the structure and properties of electrodeposited Ni”. *Materials Letters* 62: 3487-3489.
- [17] Świrad S. 2011. “The surface texture analysis after sliding burnishing with cylindrical elements”. *Wear* 271: 576-581.
- [18] Yang J., Ma R., Zhu M., Xiong Y., Shi J., Li X., Li H., Che J. 2022. “Microstructure and mechanical properties of hot-pressed SiC nanofiber reinforced SiC composites”. *Ceramics International* (available online).
- [19] [https://www.ceromit.pl/uploads/PDFy/w%C5%82asno%C5%9Bci\\_materia%C5%82%C3%B3w\\_ceramicznych.pdf](https://www.ceromit.pl/uploads/PDFy/w%C5%82asno%C5%9Bci_materia%C5%82%C3%B3w_ceramicznych.pdf) (28<sup>th</sup> Feb. 2022)